NASA Technical Memorandum 89001

NASA-TM-89001 19860022119

DEVELOPMENT OF A TAKEOFF PERFORMANCE MONITORING SYSTEM

R. Srivatsan, David R. Downing,
and Wayne H. Bryant

AUGUST 1986

National Aeronautics and
Space Administration

Langley Research Center
Hampton, Virginia 23665

DEVELOPMENT OF A TAKEOFF PERFORMANCE MONITORING SYSTEM

R. Srivatsan * and David R. Downing **
University of Kansas,
Lawrence, KS 66045.

and

Wayne H. Bryant ***
NASA Langley Research Center,
Hampton, VA 23665.

Abstract

The paper discusses the development and testing of a real-time Takeoff Performance Monitoring System. The algorithm is madeup of two segments: a pretakeoff segment and a real-time segment.

One-time inputs of ambient conditions and airplane configuration information are used in the pretakeoff segment to generate scheduled performance data for that takeoff.

The real-time segment uses the scheduled performance data generated in the pretakeoff segment, runway length data, and measured parameters to monitor the performance of the airplane throughout the takeoff roll. Airplane and engine performance deficiencies are detected and annunciated. An important feature of this algorithm is the one-time estimation of the runway rolling friction coefficient.

The algorithm was tested using a six degree of freedom airplane model in a computer simulation. Results from a series of sensitivity analysis are also included.

Nomenclature

a	Acceleration (feet/sec^2)
A_0, A_1, A_2, A_3	Coefficients of the acceleration cubic in true airspeed
C_D	Drag coefficient
C_L	Lift coefficient
D	Drag force (lbs.)
D_{RWY}	Distance along the runway (feet)
EPR	Engine pressure ratio
F	Force along an axis (lbs.)
g	Gravitational acceleration (ft/sec^2)
$\dot{H}$	Rate of change of height (ft/sec)
I_{YY}	Y-axis moment of inertia (slug-ft^2)
L	Lift Force (lbs)
L_G	Landing gear force or moment (lb or ft-lb)
m	Airplane mass (slugs)

Nomenclature (continued)

M	Pitching moment (ft-lb)
MACH	Mach number
p	Roll Rate (rad/sec)
q	Pitch Rate (rad/sec)
r	Yaw Rate (rad/sec)
S	Reference (wing) area (ft^2)
T_0, T_1, T_2, T_3	Coefficients of the thrust cubic in true airspeed
Temp	Temperature (°F or °R)
THR	Engine thrust (lbs)
u	Linear speed in the X direction (ft/sec)
$\underline{u}$	Control input vector
v	Linear speed in the Y direction (ft/sec)
v_G	Ground speed (ft/sec)
v_T	True airspeed (ft/sec)
w	Linear speed in the Z direction (ft/sec)
W	Airplane Weight (lbs)
x	any appropriate variable
$\underline{x}$	State vector
Γ	Discrete control effectiveness matrix
δ_{th}	Throttle position (deg)
ΔC_D	Incremental drag coefficient
ΔC_L	Incremental lift coefficient
ΔT	Iteration time step (sec)
$\Delta\mu$	Incremental friction coefficient
θ_B	Pitch attitude (rad)
μ	Runway rolling friction coefficient
ξ	Discrete transform multiplier
ρ	Air density (slug/ft^3)
Φ	Discrete state matrix

Superscripts

$\dot{}$	Time derivative
$\hat{}$	Estimated quantity

Subscripts

B	Body axes
brake	Due to braking
C	Command
FSP	Due to flight spoilers
GSP	Due to ground spoilers

* Aerospace Research Engineer
** Professor of Aerospace Engineering
*** Head, Systems Architecture Branch

Nomenclature (continued)

Subscripts (continued)

M Measured value
n n-th step
n+1 n+1 th step
RWY Runway
total Total force/moment
X_B Along body X-axis
Z_B Along body Z-axis

Introduction

While the percentage of initiated takeoffs that have resulted in accidents is very small, accidents in this flight phase account for about 12% of all aircraft related accidents [1]. Also, while the accident rate in all other flight phases has been decreasing in recent years, those in the takeoff phase have remained almost constant [1].

The concept of takeoff performance monitoring is nothing new. This phase of flight has been of concern since the beginning of regulated aviation operation. Several single point performance checks have been proposed [2], as well as some that deal with checking the time required to attain a prespecified speed [1].

The takeoff performance monitoring system described in this paper has the following features:

* The system is carried on the airplane and hence is airport independent.
* The system detects performance deficiencies by comparing the airplane's present performance with a nominal performance for the given conditions.
* The system computes the runway used and hence the runway available for further action.
* The system also predicts the runway required to achieve rotation speed or to bring the airplane to a complete halt.
* The system can be configured to operate in a fully automated mode.

The algorithm

At any point during the takeoff roll, the amount of runway required to achieve rotation speed is a function of the instantaneous speed of the airplane and how well it will accelerate until rotation speed. The instantaneous acceleration of the airplane is given by

$$a = \frac{THR - D - \mu (W - L)}{m} \quad - (1)$$

The thrust in the above equation is a function of airspeed and not easily estimated onboard an airplane. Drag and lift vary as the square of the airspeed. The rolling friction coefficient which depends on the runway and tire conditions is a major source of uncertainty. The airplane acceleration is seen to represent a composite measure of the performance of the airplane. A comparison of the instantaneous acceleration with a nominal value for the present airspeed is used to detect performance deficiencies.

The algorithm presesented here attempts to circumvent the difficulties associated with thrust and rolling friction coefficient estimation. It consists of two segments: a pretakeoff segment and a real-time segment. For each takeoff the pretakeoff segment is utilized to generate nominal performance data particular to that takeoff run. The real-time segment keeps track of the runway used, the runway remaining, the runway needed to achieve rotation speed, and the runway needed to bring the airplane to a complete stop. These lengths and a comparison of the actual airplane performance with the nominal value from the pretakeoff segment is used to augment the GO/ABORT decision.

The Pretakeoff Segment

The airplane acceleration performance is predicted for two extreme values of rolling friction coefficients: a low value (μ=0.005) and a high value (μ=0.040) using the inputs shown in Table 1. The algorithm consists of three parts as shown in Figure 1 and can be run off-line on the onboard computers or on ground support computers with the results downloaded to the airplane computers.

The first part performs a flight manual look-up to determine the recommended engine pressure ratio for takeoff, the decision speed, and the rotation speed. The throttle setting needed to achieve the engine pressure ratio is also computed.

The second part of this segment computes the airplane's scheduled acceleration performance as follows [3,4,5]. First the aerodynamic coefficients are extracted from the aerodynamic data base for the airplane as a function of the motion variables. The aerodynamic forces and moments are computed in the airplane stability axis system. These forces and moments are then transformed into the body axis system. The components of the engine forces and moments along the body axes are determined using the manufacturer supplied engine model. A manufacturer supplied landing gear model is utilized in computing the forces and moments generated by it along the body axis system.

Table 1: Inputs for the Pretakeoff Segment

AMBIENT CONDITIONS
Pressure Altitude
Ambient Temperature
LOADING AND CONFIGURATION INFORMATION
Airplane Weight
Center of Gravity Location
Selected Flap Setting

The resultant forces acting through the center of gravity along the body X and Z axes are obtained as

$$F_{X_{B_{total}}} = F_{X_B} + THR_{X_B} + L_{G_{X_B}} \quad - (2)$$

$$F_{Z_{B_{total}}} = F_{Z_B} + THR_{Z_B} + L_{G_{Z_B}} \quad - (3)$$

The resultant moment about the body Y-axis (the pitching moment) is given by

$$M_{B_{total}} = M_B + THR_{M_B} + L_{G_{M_B}} \quad - (4)$$

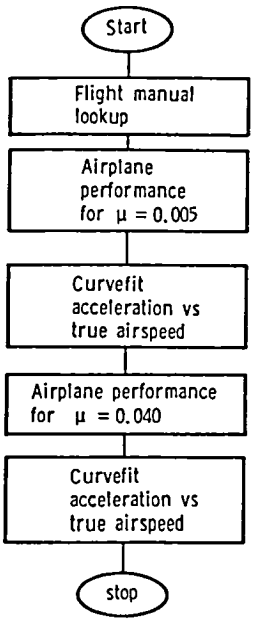

Figure 1: Block Diagram of the Pretakeoff Segment

Using these forces, moments and body X and Z components of gravitational acceleration, the airplane acceleration along the body axes as

$$\dot{u}_B = (F_{X_{B_{total}}}/m) - g \sin\theta_B + (r_B v_B - q_B w_B) \quad - (5a)$$

$$\dot{w}_B = (F_{Z_{B_{total}}}/m) - g \cos\theta_B + (q_B u_B - p_B v_B) \quad - (5b)$$

$$\dot{H}_{CG} = u_B \sin\theta - w_B \cos\theta \quad - (5c)$$

with $p_B = r_B = 0$.

The pitching moment and the body Y-axis moment of inertia are used in computing the pitch acceleration using

$$\dot{q}_B = M_{B_{total}} / I_{YY_B} \quad - (6)$$

The rate of change of pitch attitude is written as

$$\dot{\theta}_B = q_B \quad - (7)$$

The parameters ($\dot{\theta}_B$, $\dot{u}_B$, $\dot{H}_{CG}$, $\dot{w}_B$, $\dot{q}_B$, v_G) are integrated using a second order Adam-Bashworth numerical integration scheme

$$x_{n+1} = x_n + \frac{\Delta T}{2} (3 \dot{x}_n - \dot{x}_{n-1}) \quad - (8)$$

to obtain new values for (θ_B, u_B, H_{RWY}, w_B, q_B, D_{RWY}). In the above computations a nominal throttle movement time history was chosen to duplicate typical operational procedures. This throttle position serves as the input to a throttle servo with the following dynamics:

$$\delta_{th}(n\Delta T) = \xi \, \delta_{th}[(n-1)\Delta T] + (1-\xi) \, \delta_{th_C}(n\Delta T) \quad - (9)$$

The last part of this segment deals with curve fitting the along track acceleration, a, as a function of the airplane true airspeed, v_T, to generate a set of coefficients for a "nominal performance" data set for the takeoff run. A least square error cubic polynomial curvefit method [6] is utilized to generate

$$a = A_0 + A_1 v_T + A_2 v_T^2 + A_3 v_T^3 \quad - (10)$$

This process is carried out twice; once for the low friction coefficient and a second time for the high friction coefficient. Figure 2 illustrates the results obtained from the pretakeoff segment for the takeoff conditions of Table 2.

The Real-Time Segment

A block diagram of the real-time segment is shown in Figure 3. This segment performs the following functions:

1. Initially commands the throttle to the required throttle setting for takeoff
2. Monitors the engine in terms of its engine pressure ratio
3. Monitors the performance of the airplane in terms of its acceleration performance
4. Estimates the runway rolling friction coefficient
5. Predicts the runway required to achieve rotation speed
6. Predicts the runway required to stop the airplane and
7. Generates go or abort signals

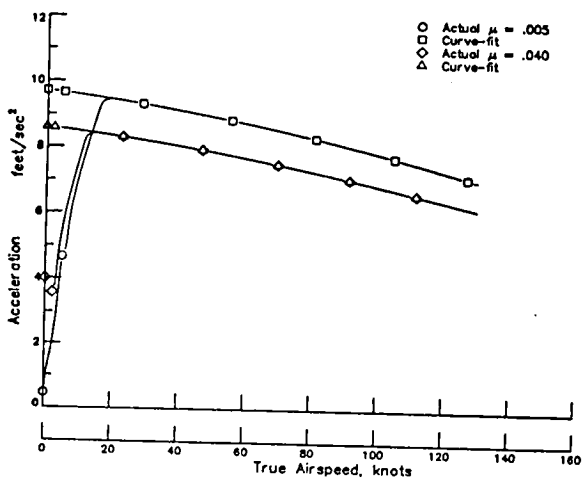

Figure 2: Acceleration Time Histories and their Curvefit from the Pretakeoff Segment

Table 2 : Flight Conditions for the Pretakeoff computations of Figure 2

Weight	88504	lbs
Center of Gravity	19% $\bar{c}$	behind LEMAC
Flap Setting	5	deg
Pressure Altitude	32	feet
Ambient Temperature	75	deg F

where LEMAC = leading edge of mean aerodynamic chord

The real-time segment requires several input parameters. Some of these are one-time inputs while others are continuously needed inputs. Table 3 lists all of these input parameters.

The pressure altitude and ambient temperature inputs are used to compute the air density, and temperature and pressure ratios (atmospheric calculations) once during the real-time segment.

Table 3: Parameters needed for the Real-Time Segment

ONE-TIME INPUTS

- Ambient Temperature
- Ambient Pressure
- Runway Wind
- Weight
- Flap Setting
- Stabilizer Setting

} Obtained from the Pretakeoff Segment

- Runway Available for Rotation
- Runway Available for Stopping
- Nominal Rolling Friction Coefficient

NEEDED CONTINUOUSLY

- Left & Right Throttle position
- Left & Right Engine Pressure Ratio
- Ground Speed
- Along Track Acceleration
- Calibrated Airspeed

The generation of a basis for scheduled performance consists of interpolating between the sets of coefficients generated in the pretakeoff segment (equation 10) to obtain a set of coefficients corresponding to the input value for nominal rolling friction coefficient (Table 3). This one-time computation gives an initial basis for performance comparisons.

Two table lookups are performed in this segment. The first lookup obtains the flight manual recommended stabilizer setting for the given airplane loading configuration. The nominal lift and drag coefficients for the present takeoff roll, increments in lift and drag coefficients with full deflection of the flight and ground spoilers are also determined. The other lookup function is identical to the one in the pretakeoff segment.

Values for the continuously needed parameters are supplied by sensors on the airplane. Before use by the system these sensor outputs are processed through a filter implementation. The measured acceleration and ground speed are processed through a second order complementary filter to estimate the bias present in the acceleration signal as follows [3,7]:

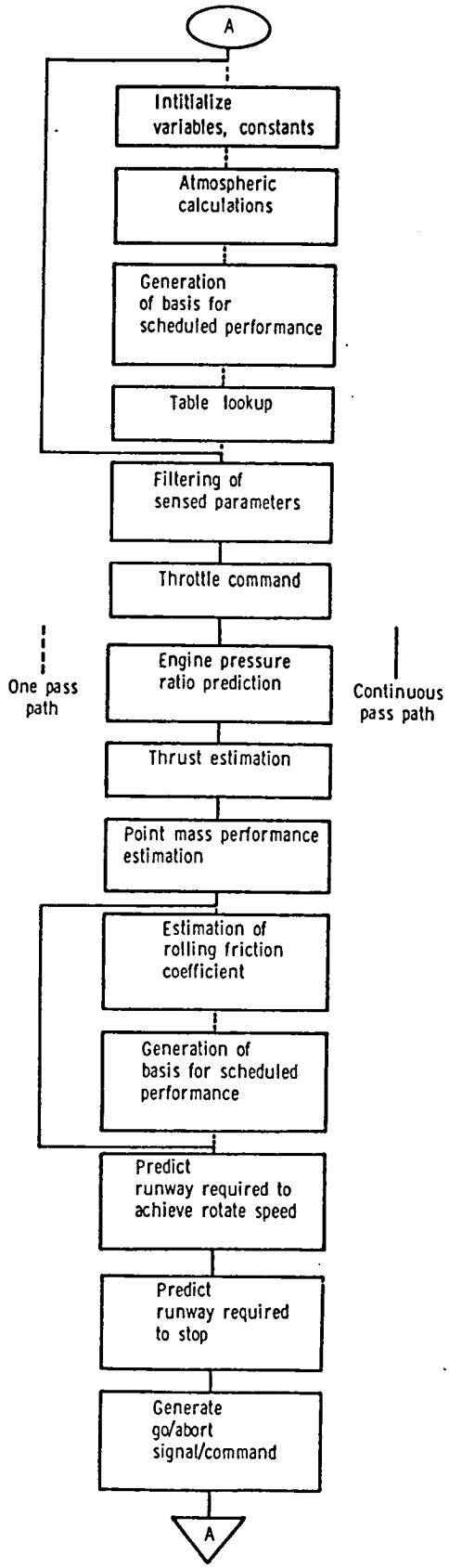

Figure 3: Block Diagram of the Real-time Segment

$$\underline{x}_{n+1} = \Phi \underline{x}_n + \Gamma \underline{u}_n \quad - (11a)$$

where

$$\underline{x} = \begin{bmatrix} x(1) \\ x(2) \end{bmatrix}$$

$$\underline{u} = \begin{bmatrix} v_G \\ a_M \end{bmatrix}$$

$$\hat{v}_G = x(1) \quad - (11b)$$

$$a_{F1} = a_M + x(2) \quad - (11c)$$

The acceleration output from the complementary filter (a_{F1}), measured values of engine pressure ratio (left & right), and calibrated airspeed are passed through a first order lag filter [3,8] to remove noise and the outputs from this filter are the values used by the system.

The throttle command block generates a throttle movement history identical to the one used in the pretakeoff segment.

An empirical model of the steady state behavior of the engine pressure ratio and thrust is extracted from the manufacturer supplied engine model to predict these parameters as follows:

$$\hat{EPR}_{\substack{left \\ right}} = f\left(\delta_{th_{\substack{left \\ right}}}, Temp_{total}\right) \quad - (12)$$

$$\hat{THR}_{\substack{left \\ right}} = f\left(\hat{EPR}_{\substack{left \\ right}}, \hat{MACH}\right) \quad - (13)$$

A point mass formulation of the equations of motion is used to estimate the performance of the airplane [3,9]. First the wind speed and measured ground speed are combined to obtain true airspeed, mach number and dynamic pressure. The nominal lift and drag coefficients yield the lift and drag forces. Combining these with the weight and rolling friction coefficient (input value), and the estimated thrust (based on measured engine pressure ratio) results in an estimated airplane acceleration. The measured ground speed is numerically integrated (rectangular integration) to obtain distance along the runway.

One salient feature of this algorithm is the estimation of the runway friction coefficient in real-time. This is a single point estimate carried out a few seconds (10 seconds in this implementation) into the takeoff run. The estimation takes place as follows. First, the thrust is represented as a cubic in airspeed

$$THR = T_0 + T_1 v_T + T_2 v_T^2 + T_3 v_T^3 \quad - (14)$$

At any true airspeed, the acceleration corresponding to two rolling friction coefficients can be written as

$$\hat{a} = g((T_0 - \hat{\mu}_1 W) + T_1 v_T + (T_2 - \tfrac{1}{2}\rho S C_D + \tfrac{1}{2}\hat{\mu}_1 \rho S C_L) v_T^2 + T_3 v_T^3) / W \quad - (15a)$$

$$a = g((T_0 - \hat{\mu}_2 W) + T_1 v_T + (T_2 - \tfrac{1}{2}\rho S C_D + \tfrac{1}{2}\hat{\mu}_2 \rho S C_L) v_T^2 + T_3 v_T^3) / W \quad - (15b)$$

Subtracting a from $\hat{a}$ and solving for the difference in friction coefficients

$$\Delta\hat{\mu} = \hat{\mu}_2 - \hat{\mu}_1 = (\hat{a} - a) / (g (W - \tfrac{1}{2}\rho S C_L v_T^2) / W) \quad - (16)$$

where

$\hat{\mu}_2$ = estimate of the actual runway friction coefficient

$\hat{\mu}_1$ = assumed friction coefficient

$\Delta\hat{\mu}$ = estimated difference in the friction coefficients

Thus the actual rolling friction coefficient is estimated as

$$\hat{\mu}_2 = \hat{\mu}_1 + \Delta\hat{\mu} \quad - (17)$$

Immediately after this process the basis for scheduled performance is recomputed with $\hat{\mu}_2$ as the present estimate of the friction coefficient.

The runway required to achieve rotation speed is computed by a ten step rectangular integration scheme between the present true airspeed and the true airspeed for rotation. The acceleration in each interval is assumed to remain constant at a value given by the scheduled performance basis for the true airspeed at the midpoint of the interval.

To calculate the stopping distance, the system simulates the effect of a series of commands to deploy the flight and ground spoilers, to reduce the throttle to an idle setting, and to apply full braking. The computations are based on the following assumptions.

1. The flight and ground spoilers are commanded through servos modelled as first order lags.
2. With full braking the rolling friction coefficient is increased by a constant amount over the prevalent value.
3. Maximum wheel braking is achieved in a ramp fashion per given time period.
4. Thrust is assumed to vary linearly from the present value to idle thrust with throttle position (reaching idle thrust for a throttle position of zero).
5. Changes in lift and drag coefficients produced by flight and ground spoilers are assumed to vary linearly with deflection.

Using these assumptions in a numerical integration scheme based on incremental time the stopping distance is computed in a point mass formulation with the lift and drag coefficients computed as

$$C_L = C_{L_{nominal}} + \Delta C_{L_{FSP}} + \Delta C_{L_{GSP}} \quad - (18a)$$

$$C_D = C_{D_{nominal}} + \Delta C_{D_{FSP}} + \Delta C_{D_{GSP}} \quad - (18b)$$

and the friction coefficient as

$$\mu = \mu_{nominal} + \Delta\mu_{brake} \quad - (18c)$$

Generation of GO/ABORT signal

The engine pressure ratio is used as a check on engine health. After allowing time for the engine transients to die out, the measured value is compared with the predicted value (corresponding to the measured throttle position).

If this difference is more than a preselected limit an engine failure flag is set.

$$\frac{|EPR_{1/r} - \hat{EPR}_{1/r}|}{EPR_{1/r}} > EPR_{error\ limit}$$

$$\Rightarrow \text{Eng. Fail}_{1/r} \quad - (19)$$

At any time after the rolling friction coefficient is estimated, any difference between the measured and the predicted accelerations exceeding a preselected limit causes a performance failure flag to be set.

$$\frac{|a - \hat{a}|}{a} > a_{error\ limit}$$

$$\Rightarrow \text{PER. Fail} \quad - (20)$$

With these flags, the following conditions result in a Go signal:

1. No engine failure flag or performance failure flag is set and the runway length available is greater than the runway length required to achieve rotation speed.
2. Only one engine failure flag is set and the runway remaining is less than that required for stopping the airplane.
3. Performance failure flag is set without either engine failure flag being set and there is insufficient runway length for stopping.

The following conditions result in an Abort signal:

1. Runway length available for achieving rotation speed is less than that required.
2. Both the engine failure flags are set.
3. One engine failure flag is set and there is sufficient runway length available for stopping.
4. Performance failure flag is set and sufficient runway length is available for stopping.

Testing

The algorithm described in the above sections was specialized for the NASA Transport Systems Research Vehicle (TSRV) B-737 twin jet airplane and evaluated using the six degree-of-freedom batch simulation model running at twenty times a second. The simulation utilizes a pseudo random number generator to superimpose zero mean Gaussian noise signals with any chosen standard deviations on any of the sensed parameters. Table 4 lists the sensed parameters used for this check out along with their corresponding standard deviations and biases.

The pretakeoff computations use an iteration time step of .05 second. The computations of this segment are carried out prior to the start of the batch simulation of the TSRV B-737.

The takeoff performance monitoring system is called ten times a second, or every other iteration cycle from the TSRV B-737 batch simulation. Some of the parameters used in this segment are as follows.

ΔT = 0.1 second

$\Delta\mu_{brake_{max}}$ = 0.45

$t_{ramp_{brake}}$ = 0.6 second

$EPR_{error\ limit}$ = 0.15

$a_{error\ limit}$ = 0.15

Table 4: Sensor Noise and Bias Characteristics

All noises are Gaussian with standard deviations as indicated below.

PARAMETER	SIGMA	BIAS
Along trck Acceleration	0.32	0.32
Pressure Altitude (ft)	0.0	0.0
Calib. Airspeed (kts)	2.0	0.0
True Airspeed (kts)	2.0	4.0
Throttle Pos. (deg)	0.2	-0.4
Engine Pressure Ratio	0.01	0.02
Engine N1 RPM	0.01	0.01
Exhaust Gas Temp.(°F)	0.01	0.01
Fuel Flow Rate (lb/hr)	0.01	0.02

SIGMA - Standard Deviation
BIAS - Constant Bias Value

Normal Takeoff Test Cases

Ten cases are presented to demonstrate the normal performance of the algorithm. These cases, listed in Table 5, represent different combinations of loading and ambient conditions. An actual airplane under these conditions would have gone through a successful ground roll and rotation.

Table 5: Normal Takeoff Test Cases

CASE	PRESSURE ALTITUDE feet	TEMP. ° F	RWY WIND knots	WEIGHT lbs	FR. COEFF.
I	32.	75.0	0.	88504.	.015
II	0.	75.	0.	88504.	.015
III	100.	75.	0.	88504.	.015
IV	32.	0.	0.	88504.	.015
V	32.	100.	0.	88504.	.015
VI	32.	75.	10.	88504.	.015
VII	32.	75.	20.	88504.	.015
VIII	32.	75.	0.	88504.	.025
IX	32.	75.	0.	88504.	.007
X	32.	75.	0.	98000.	.015

Table 6 summarizes the results obtained for the cases listed in Table 5. The second column shows the measured calibrated airspeed at rotation (more precisely the instant at which the simulation was terminated as having achieved rotation speed). The prediction error in column four of this table is the amount by which the runway requirement prediction was in error. A negative number in this column indicates that the airplane used that much more runway than was predicted by the algorithm. It is seen that this error is less than 5% of the runway used. The last column shows the updated friction coefficient after 10 seconds into the takeoff run. This is the algorithm estimated friction coefficient for that takeoff run as opposed to the actual value

(column six of table 5). Figure 4 shows time histories of the predicted runway requirements and the runway used for case I of Table 5. Also shown in this plot is the sum of the two instantaneous values. This line measures the "goodness" of the algorithm prediction. For a good runway length predictor, this line should remain a horizontal straight line i.e., at any given instant the predicted runway required to achieve rotation speed is equal to the prediction at any previous time minus the runway used between the two points. The downward shift in the runway required curve and the consequent shift in the sum is caused by the estimation of friction coefficient at 10 seconds.

Engine Malfunction Test Cases

Two types of engine malfunctions are simulated for this study, as listed below:

1) Engine does not develop hand book EPRs
2) Engine does not develop hand book thrust

For the first case the the EPRs in the simulation are forced to 15% above and below their nominal values. For both, the above and below nominal EPR cases an engine failure flag was set at the 10 second mark.

Table 6: Summary of results for cases in Table 5

CASE	MEASURED CAS @ rotatn	RUNWAY USED	RUNWAY PRED. ERROR	UPDATED FRICTION COEFF.
I	128.1	3262.	-130.	.017
II	128.3	3266.	-142.	.017
III	128.6	3277.	-128.	.017
IV	129.1	2740.	-58.	.017
V	129.4	3603.	+22.	.018
VI	129.1	2685.	+5.	.017
VII	128.8	2300.	-11.	.018
VIII	128.2	3272.	-26.	.027
IX	128.1	3085.	-40.	.009
X	138.1	4155.	-13.	.017

Engine thrust malfunction is simulated by forcing the thrust to 15% above and below the nominal value. It is assumed that the thrust degradation does not affect the EPRs. The EPR output from the engine still corresponds to the nominal value. Since the EPR is the only parameter used for engine health check, neither case results in an engine failure flag. At the 10 second point the difference in between the measured and predicted accelerations is attributed to a faulty friction coefficient input. For the 115% thrust case this results in an updated friction coefficient of -0.028 (changed from 0.015) and for the 85% thrust case the updated friction coefficient is 0.063. These values are well out of the nominal range of 0.015 to 0.040 .

Sensitivity and Failure Mode Analysis

Sensitivity of the algorithm to input errors and the effects of sensor failures are considered here. The sensitivity analysis is carried out by forcing selected inputs to the algorithm and the simulation to be different and comparing the algorithm's predictions with the true values generated by the simulation. The failure analysis is carried out by causing the sensor outputs from the simulation model to be in error and again comparing the predictions with performance.

Case I of Table 5 serves as the baseline for all the analyses of this section. In addition, the baseline flap setting is 5 degrees.

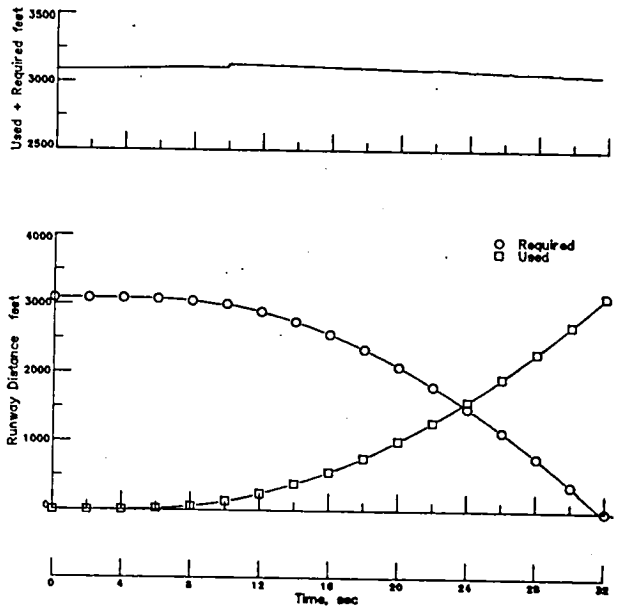

Figure 4: Plots of Runway Required and Used for Case I of Table 5

Sensitivity to errors in inputs

The first parameter considered is runway winds. The algorithm and the simulation are forced to use different runway wind conditions. The results are summarized in Table 7. It is seen that the algorithm is highly sensitive to errors in runway winds. No abort signal is generated by the algorithm. At the 10 second point, the difference between the predicted and measured acceleration is used to generate a friction coefficient value which in several cases is quite different from the actual value. An onboard wind estimator is considered in an effort to reduce this sensitivity. The runway winds are estimated as being the difference between the measured and algorithm computed calibrated airspeed prior to estimating the friction coefficient, as a one time operation. The prediction error changed from -1058 feet without a wind estimator to -139 feet (assumed head wind of 20 knots versus an actual no wind condition).

It is seen from Table 8 that the algorithm is sensitive to errors in ambient temperature inputs. Even though the estimated friction coefficient is not appreciably different from the actual value, the error in the runway requirements increases to about 10% of the total used.

The effect of errors in gross weight input are summarized in Table 9. Even though the error in the predicted runway requirements is rather small, the adjusted friction coefficient is seen to be very much different from the actual value of 0.015 . The difference between the measured and predicted accelerations caused by the weight error is treated as being caused by a friction coefficient discrepancy at the 10 second mark. The other problem with this situation is that the airplane rotation speed is based on the 88504 lb

weight and thus results in a premature rotation for the over weight case. In the under weight case the airplane will remain on the runway longer than needed.

Table 7: Effect of Wind Speed Error

WIND SPEED		PERFORMANCE		
ASSUMED (knots)	ACTUAL (knots)	ADJUSTED μ	RWY PRED. ERROR (feet)	Δ PRED. ERROR (feet)
10.	0.	.012	-615.	-620.
10.	10.	.017	5.	0.*
10.	20.	0.022	447.	442.
20.	0.	.007	-1058.	-1046.
20.	10.	.012	-444.	-432.
20.	20.	.017	-12.	0.*
20.	30.	.023	428.	440.

* nominal case

Table 8: Effect of Ambient Temperature Errors

TEMPERATURE		PERFORMANCE		
ASSUMED °F	ACTUAL °F	ADJUSTED μ	RWY PRED. ERROR (feet)	Δ PRED. ERROR (feet)
50.	25.	.017	347.	348.
50.	50.	.017	-40.	0.*
50.	75.	.017	-505.	-465.

* nominal case

Table 9: Effect of Gross Weight Errors

WEIGHT		PERFORMANCE		
ASSUMED (lbs)	ACTUAL (lbs)	ADJUSTED μ	RWY PRED. ERROR (feet)	Δ PRED. ERROR (feet)
88504.	78504.	-.021	-55.	75.
88504.	88504.	.017	-130.	0.*
88504.	98504.	.048	61.	191.

* nominal case

Effects of flap setting errors are summarized in Table 10. The ruway prediction errors are seen to be small for the chosen rotation speed. But again the chosen rotation speeds are based on the wrong flap setting. In addition, the high actual flap setting is also seen to result in a very low friction coefficient estimate.

Sensitivity to aerodynamic degradation

Table 11 summarizes the effects of aerodynamic degradation such as caused by ice formation on the wings. The two cases explored are a 10% reduction in lift accompanied by a 10% increase in drag and a 15% degradation. In both the cases the friction coefficient is adjusted in a minor way to bring the runway length predictions very close to nominal.

Effects of reduced frequency of calls to the takeoff performance algorithm are shown in Table 12. At 5 calls per second, the friction coefficient is seen to be adjusted to a rather low value. The prediction error goes to just over 5% of the total runway used.

Table 10: Effect of Flap Setting Errors

FLAP SETTING		PERFORMANCE		
ASSUMED (deg)	ACTUAL (deg)	ADJUSTED μ	RWY PRED. ERROR (feet)	Δ PRED. ERROR (feet)
5.	1.	.017	-155.	-25.
5.	5.	.017	-130.	0.*
5.	15.	.002	-144.	-14.

* nominal case

Failure Analysis

Effects of accelerometer biases are shown in Table 13. The algorithm is seen to be able to handle accelerometer biases of at least ± 2 feet/sec/sec over the nominal value with out significant changes to the friction coefficient or the runway prediction.

The effect of a 15% scaling of the accelerometer is shown in Table 14. This caused a significant change in the estimated friction coefficient. The runway prediction error is increased to just over 5% for the 115% accelerometer scaling case.

Introducing a bias of -0.3 in the engine pressure ratio measurement (16% of an EPR of 2.0 subtracted from the nominal bias of 0.02) caused an engine failure flag to be set. A bias of +0.34 also has a similar effect.

Table 11: Effects of Aeodynamic Degradation

DEGRADATION LEVEL	PERFORMANCE		
	ADJUSTED μ	RWY PRED. ERROR (feet)	Δ PRED. ERROR (feet)
0	.017	-130.	0.*
10%	.018	-140.	-10.
15%	.018	-156.	-26.

* nominal case

Table 12: Effects of reduced calls to the algorithm

FREQUENCY OF CALLS	PERFORMANCE		
	ADJUSTED μ	RWY PRED. ERROR (feet)	Δ PRED. ERROR (feet)
10	.017	-130.	0.*
5	.002	-205.	-75.

* nominal case

Introducing a scale factor error of 15% on the engine pressure ratio measurement on either side of nominal caused engine failure flags to be set.

Forcing the ground speed sensor output to 0, 100 feet/sec, and 250 feet/sec caused a performance failure flag to be set.

Table 13: Effects Accelerometer Biases

ACCELEROMETER BIAS	PERFORMANCE		
	ADJUSTED μ	RWY PRED. ERROR (feet)	Δ PRED. ERROR (feet)
2.32	.016	-150.	-20.
0.32	.017	-130.	0.*
-1.68	.017	-130.	0.

* nominal case

Table 14: Effects Accelerometer Scaling

ACCELEROMETER SCALE FACTOR	PERFORMANCE		
	ADJUSTED μ	RWY PRED. ERROR (feet)	Δ PRED. ERROR (feet)
85%	.029	7.	137.
100%	.017	-130.	0.*
115%	.006	-253.	-123.

* nominal case

Concluding Remarks

A Takeoff Performance Monitoring System has been developed and tested using a batch simulation of the NASA TSRV B-737 airplane. Ten normal takeoff cases were used in testing the algorithm. The runway required was found to be predicted within 5% of the overall runway used.

Engine malfunctions that affected the engine pressure ratio were detected and engine failure flags were raised.

Sensitivity analysis indicates that the algorithm is highly sensitive to errors in runway wind inputs. An onboard wind estimator reduces this sensitivity. The algorithm is also sensitive to errors in ambient temperature inputs. Errors in weight inputs were found to cause the runway friction coefficient to be adjusted to unreasonable values. Errors in flap setting were accounted for by changing the friction coefficient but the rotation speed was based on the erroneous flap setting input. Aerodynamic degradations of 10 and 15% did not cause any problems. Frequency of calls to the algorithm could not be halved (changed from the 10 calls per second to 5 calls per second).

The algorithm has the capability to adjust for accelerometer bias and scale factor errors. Engine Pressure Ratio biases of 15% of nominal and 15% scale factors caused engine failure flags to be raised. Failed ground speed sensors raised a performance failure flag.

The errors associated with inputs could be eliminated for the most part by automating these inputs.

The algorithm looks viable.

It is currently being implemented in a real-time simulator at NASA Langley Research Center and will be evaluated by pilots.

References

1. Minutes of the first meeting of the SAE Take-off Performance Monitoring Ad Hoc Committee of the Aircraft Division of the Aerospace Council; May 15-16, 1984, Washington, DC.
2. Small, Maj. J.T.; Feasibility of using longitudinal acceleration (N_x) for monitoring takeoff and stopping performance from the cockpit; Proceedings of the Twenty-seventh Symposium, Beverly Hills, CA, September28 - October 1, 1983, (A84-16157 05-05).
3. Srivatsan, R.; Design of a Takeoff Performance Monitoring System; Doctoral dissertation, University of Kansas; June, 1985.
4. Etkin, Bernard; Dynamics of Atmospheric Flight; John Wiley & Sons.
5. Roskam, Jan; Airplane Flight Dynamics and Automatic Flight Controls Part - I; Roskam Aviation and Engineering Corp.; 1979.
6. Central Computing Complex Document N-3; Mathematical and Statistical Software at Langley; NASA Langley Research Center; April 1984.
7. Pines, Samuel; Terminal Area Automatic Navigation, Guidance, and Control Research Using the Microwave Landing System (MLS): Part 2-RNAV/MLS Transition Problems for Aircraft; NASA CR 3511; January 1982.
8. Franklin, G.F.; Powell, J.D.; Digital Control of Dynamic Systems; Addison-Wesley; June 1981.
9. Lan, C-T. E.; Roskam, J.; Airplane Aerodynamics and Performance; Roskam Aviation and Engineering Corp.; 1981.

1. Report No.	2. Government Accession No.	3. Recipient's Catalog No.
NASA TM-89001		

4. Title and Subtitle	5. Report Date
Development of a Takeoff Performance Monitoring System	August 1986
	6. Performing Organization Code: 505-66-41-05

7. Author(s)	8. Performing Organization Report No.
Raghavachari Srivatsan, David R. Downing, and Wayne H. Bryant	
	10. Work Unit No.

9. Performing Organization Name and Address	11. Contract or Grant No.
NASA Langley Research Center Hampton, VA 23665-5225	

12. Sponsoring Agency Name and Address	13. Type of Report and Period Covered
National Aeronautics and Space Administration Washington, DC 20546	TECHNICAL MEMORANDUM
	14. Sponsoring Agency Code

15. Supplementary Notes: Raghavachari Srivatsan and David R. Downing, University of Kansas, Lawrence, Kansas; and Wayne H. Bryant, Langley Research Center, Hampton, Virginia. Presented at the AIAA Guidance, Navigation and Control Conference, Williamsburg, Virginia, August 18-20, 1986.

16. Abstract

The paper discusses the development and testing of a real-time takeoff performance monitoring system. The algorithm is madeup of two segments: a pretakeoff segment and a real-time segment.

One-time inputs of ambient conditions and airplane configuration information are used in the pretakeoff segment to generate scheduled performance data for that takeoff.

The real-time segment uses the scheduled performance data generated in the pretakeoff segment, runway length data, and measured parameters to monitor the performance of the airplane throughout the takeoff roll. Airplane and engine performance deficiencies are detected and annunciated. An important feature of this algorithm is the one-time estimation of the runway rolling friction coefficient.

The algorithm was tested using a six-degrees-of-freedom airplane model in a computer simulation. Results from a series of sensitivity analysis are also included.

17. Key Words (Suggested by Author(s))	18. Distribution Statement
airplane takeoff performance acceleration runway friction pretakeoff real time	UNCLASSIFIED - UNLIMITED SUBJECT CATEGORY 08

19. Security Classif. (of this report)	20. Security Classif. (of this page)	21. No. of Pages	22. Price
UNCLASSIFIED	UNCLASSIFIED	10	A02

For sale by the National Technical Information Service, Springfield, Virginia 22161